

# COMPUTER MODELLING AND DESIGN OF CAPACITIVE SENSORS

**S.H. Khan, K.T.V. Grattan and L. Finkelstein**

Measurement and Instrumentation Centre

Department of Electrical, Electronic and Information Engineering, City University  
Northampton Square, London EC1V 0HB, UK

*Abstract: This paper presents the use of numerical finite element (FE) technique for modelling and design of capacitive sensors. The general mathematical approach to FE modelling and design of capacitive sensors is established. Two case studies are considered to show the versatility and efficiency of the developed modelling methodologies. The first involves a multielectrode capacitive sensor for two-phase flow imaging and the second – a robust capacitive angular position sensor. It is shown that although these sensors are used in very different applications, the same modelling strategies are applicable to both cases. Results are presented in terms of sensor performance characteristics for various design parameters and operational regimes. Modelling results are compared with experimental data to validate the adopted modelling strategies.*

*Keywords: Capacitive Sensors, Finite Element Modelling, Sensor Design*

## 1 INTRODUCTION

As the heart of measurement systems capacitive sensors are extensively used in many applications for measuring displacement, pressure, torque, flow, and other physical quantities [1-5]. In all these cases the primary sensor is based on the well-known capacitive technique in which the capacitance in a system of electrodes is changed owing to the redistribution of electric field caused by changes in dielectric properties and/or geometric parameters of the sensor.

In general, the performance of a capacitive sensor is dependent upon the electric field distribution between its electrodes which, in turn, depends upon its design parameters and operational regimes (e.g. flow measurement). Consequently, accurate modelling and computation of field distribution is vitally important in order to be able to design sensors that would deliver the required output characteristics. This paper presents a generic approach to modelling and CAD of capacitive sensors and validates the adopted modelling strategies by considering two case studies – capacitive sensors for flow imaging and angular position sensing.

## 2 GENERIC MODELLING STRATEGIES FOR CAPACITIVE SENSORS

As shown in Figure 1 the heuristic procedure for FE modelling and design of capacitive sensors comprises three main processes. These are the process of defining and setting up appropriate FE models (pre-processor), the process of solving the defining differential equation (solution-processor), and the process of calculating the necessary output parameters from the solution of the defining equation (post-processor). This procedure is repeated until a satisfactory design is obtained.

For capacitive sensors the defining differential equation is given by the following Laplace's equation [6] which governs the electric field distribution in the problem domain  $\Omega$  of the sensor:

$$\nabla \times \epsilon \nabla \Phi = 0 \quad \text{in } \Omega \quad (1)$$

Under appropriate boundary conditions the above equation is solved by finite element method (FEM) [7] in terms of electric potential  $\Phi$  for given permittivity distribution  $\epsilon$ . For this, in most cases it is possible to limit the problem domain to 2D region  $\Omega(x, y)$  by neglecting any leakage flux or fringing field effects due to the finite length of electrodes. This is especially true for cylindrical arrangements of sensor electrodes with small length to diameter ratio and in sensors where special measures are taken to reduce leakage field effects. In most cases it is also assumed that dielectric materials are linear, piece-wise homogeneous and isotropic. In the presence of charge densities  $\rho$  the right hand side of equation (1) is non-zero and the corresponding Poisson's equation  $\nabla \cdot \epsilon \nabla \Phi = -\rho$  is solved.

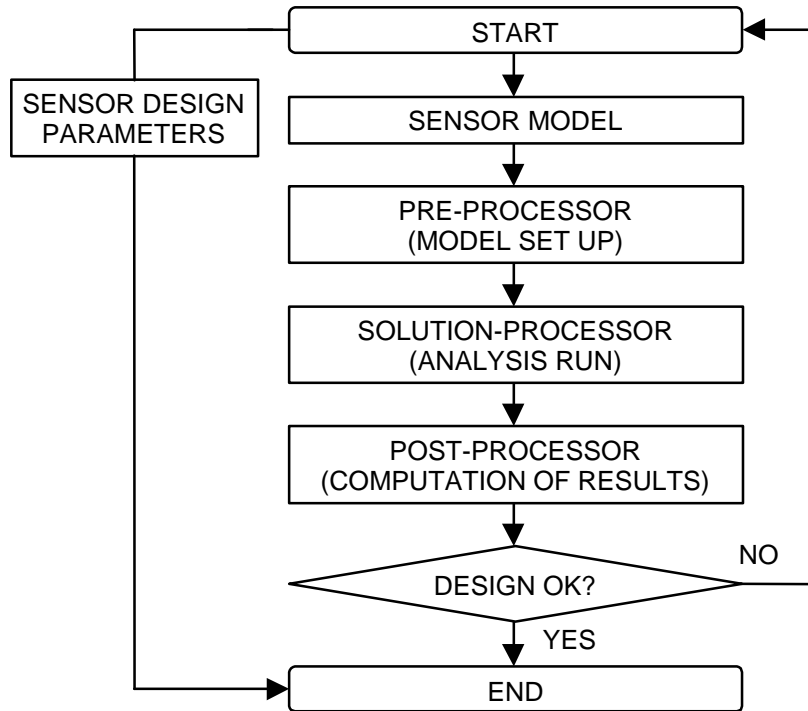


**Figure 1.** Heuristic sensor design procedure for capacitive sensors

Following the solution of equation (1), field intensity and flux density vectors  $E$  and  $D$ , and other quantities like capacitance are calculated. The FE modelling results are normally validated against experimental data. However the accuracy of results may also be verified and evaluated qualitatively and quantitatively by using special numerical techniques [8].

Since the performance modelling and CAD of capacitive sensors by FE field modelling comprises many simulation 'runs' involving model definition and discretisation, mesh refinement, parameter calculation and error estimation, validation and performance prediction, a systematic modelling approach based on effective modelling methodologies must be adopted. This is to reduce the considerable amount of time and effort needed for simulation studies and to ensure increased accuracy, reliability and comparability of simulation results. For capacitive sensors this may involve the exploitation of any symmetry conditions, reduction of problem domain, adoption of systematic model development and refinement strategies for pre-processing, full automation of analysis 'runs' and post-processing of results, etc.

### 3 CASE STUDIES - CAPACITIVE SENSORS FOR FLOW IMAGING AND ANGULAR POSITION SENSING

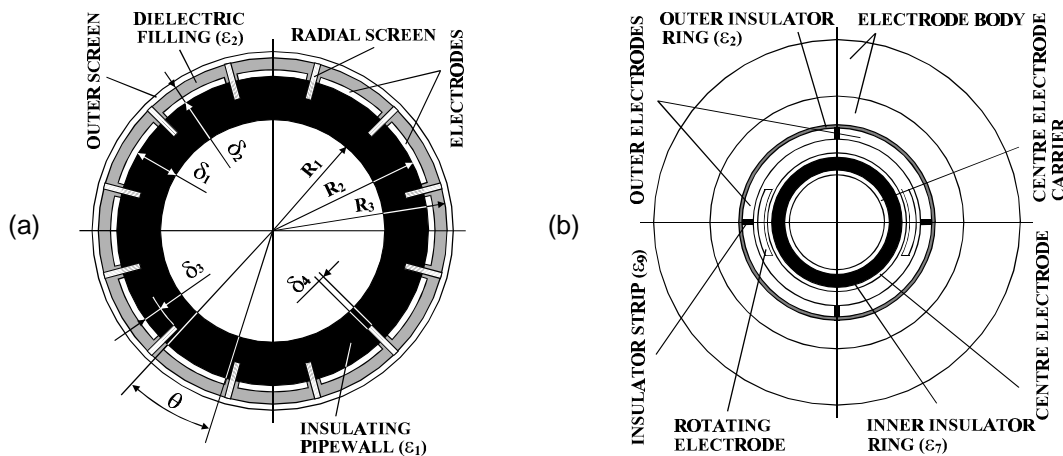


**Figure 2.** Cross sections of capacitive sensors investigated: (a) 12-electrode electrical capacitive tomography (ECT) sensor for two-phase flow imaging, (b) 4-electrode angular position sensor.

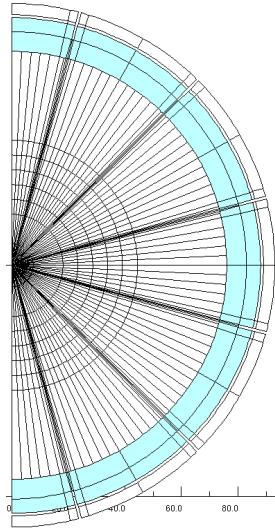


**Figure 3.** Typical finite element model of the 12-electrode ECT sensor for flow imaging shown in Figure 2(a) (half model).

The modelling strategies discussed above were used to investigate and design two capacitive sensors shown in Figure 2. Figure 2(a) shows the cross-section of a 12-electrode electrical capacitive tomography (ECT) sensor for two-phase flow imaging in real time. It consists of 12 capacitive electrodes mounted symmetrically on the surface of the special insulating section of a pipeline. The earthed radial screens reduce large capacitances between adjacent electrodes and the outer screen (also earthed) - shields stray fields. The spatial distribution of flow components inside the flow pipe is determined by measuring the capacitances between all possible combination of electrodes and solving the appropriate inverse problem. This is done by applying a constant potential to one of the electrodes and measuring the capacitances between this and the rest of the electrodes. The process is repeated for all electrodes and the capacitance data, thus obtained together with field computation results are used to solve the inverse problem and image the flow component distribution. Beck *et al* first proposed to use the capacitive technique for flow imaging [9] and today ECT has shown considerable potential to be used in industrial tomography for measurement and imaging of various processes in process industry, especially the oil industry. The performance of such an ECT sensor is strongly dependent upon its main design parameters  $\delta_1$ ,  $\delta_2$ ,  $\delta_3$ ,  $\delta_4$ ,  $\theta$ ,  $\epsilon_1$ ,  $\epsilon_2$  and number of electrodes  $N$  shown in Figure 2(a). Using the modelling strategies mentioned in the previous Section extensive simulation studies were undertaken to design and optimise the above ECT sensor against these design parameters. The resulting industrial prototype was successfully tested and shown to give improved spatial resolution (2%) and better image quality [10].

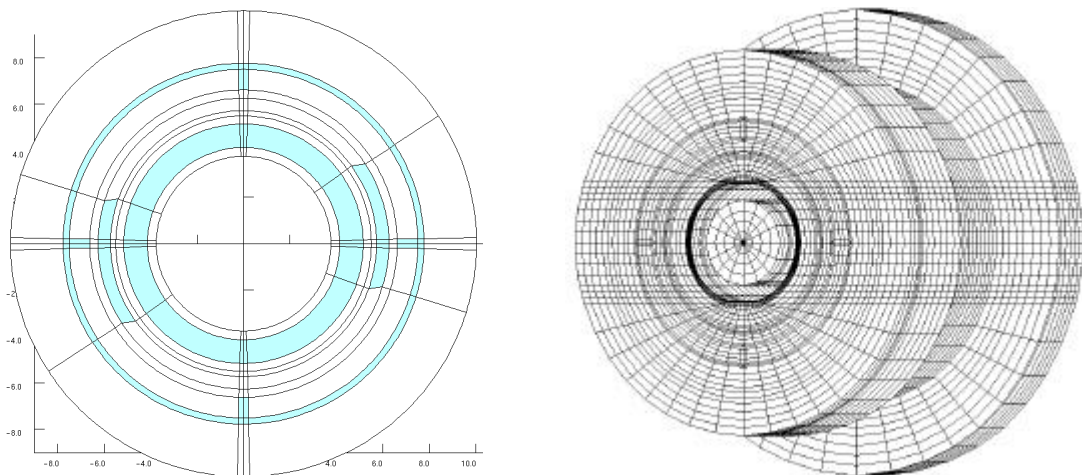


**Figure 4.** Typical 2D (a) and 3D (b) finite element model of the 4-electrode capacitive angular position sensor shown in Figure 2(b) (full models).

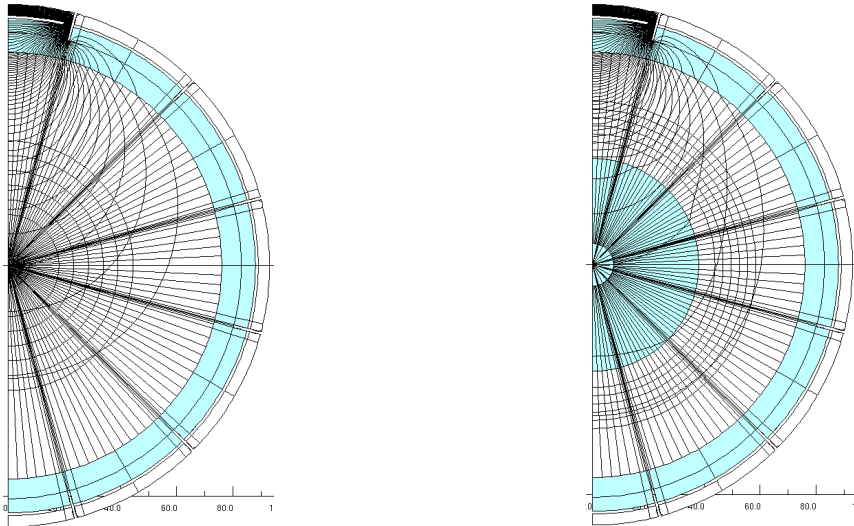


**Figure 5.** Equipotential contours in the 12-electrode ECT sensor showing the effects of (a) radial screens and (b) core flow ( $\beta=25\%$ ) on field distribution between the sensor electrodes ( $\delta_1=12$  mm,  $\delta_2=5$  mm,  $\delta_3=5$  mm,  $\delta_4=2$  mm).

The capacitive sensor shown in Figure 2(b) is used for angular position sensing in limited angle torque motors for frame scanning in infrared thermal imaging devices. It consists of a compact arrangement of four outer electrodes, one cylindrical centre electrode and two rotating electrodes. Potentials of the same magnitude but opposite polarities are given to the outer electrodes while the rotating electrodes are kept at zero potential. The rotating electrodes attached to the motor shaft rotate to change the effective overlap (and hence the field distribution) between the centre and outer electrodes. This changes the capacitance between the electrodes and also the sensor output voltage  $V$  measured between the 'floating' centre electrode and the virtual earth. Here the main design variables are the geometric parameters of the electrodes and the dielectric material  $\epsilon_r$ , and the output of interest is the magnitude and linearity of the voltage to angular position ( $V-\theta$ ) characteristic. The same modelling methodologies were used to carry out both 2D and 3D simulation studies to investigate the effects of various design parameters and leakage flux on the performance of this large diameter to length ratio sensor. The modelling results were validated against experimental data obtained from industry.

#### 4 REALISATION OF FINITE ELEMENT MODELS

Typical FE models for capacitive sensors described above are shown in Figures 3 and 4. In most cases it is usually sufficient to use 2D models for CAD and simulation studies. There are, however

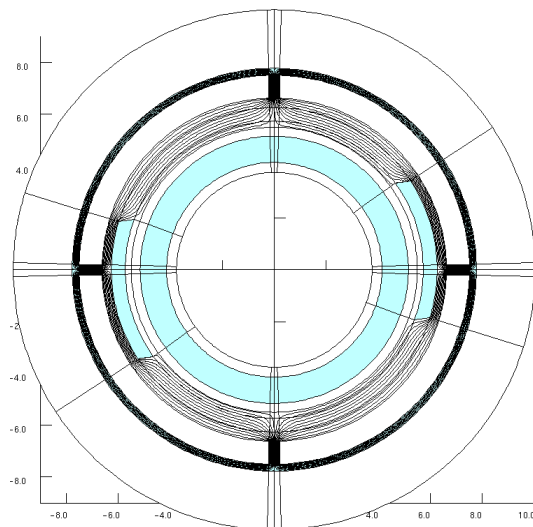


**Figure 6.** Equipotential contours in the 4-electrode angular position sensor showing field distribution between the outer and centre electrodes for position  $\theta = 8^\circ$ .

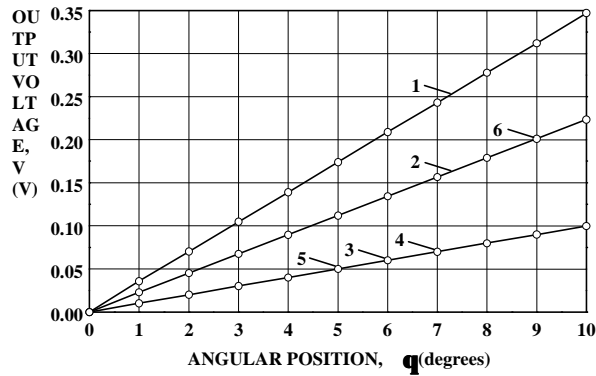


**Figure 7.** Variation of output voltage with angular position for the 4-electrode angular position sensor showing the effects of permittivities of dielectric materials in the sensor: **1**–  $\epsilon_7=1, \epsilon_2=\epsilon_9=1$ ; **2**–  $\epsilon_7=3, \epsilon_2=\epsilon_9=1$ ; **3**–  $\epsilon_7=10, \epsilon_2=\epsilon_9=1$ ; **4**–  $\epsilon_7=10, \epsilon_2=\epsilon_9=3$ ; **5**–  $\epsilon_7=10, \epsilon_2=\epsilon_9=10$ ; **6**–  $\epsilon_7=3, \epsilon_2=\epsilon_9=10$ ;

cases in which 3D models are required in order to take into account fully the complex nature of electric field distribution, especially in devices with complicated geometric configuration [11]. In addition, sometimes 3D models are also required to justify, both qualitatively and quantitatively, the use of 2D models for simulation. Such a 3D FE model for the small length-to-diameter ratio angular position sensor is shown Figure 4(b). It contains about 75000 eight-noded hexahedral elements made up of approximately the same number of nodes. For a relatively small size sensor (about 25 mm in length and 17 mm in diameter) this provides modelling accuracy comparable to that of accurate 2D models. Such 3D models were used to investigate the effects of leakage flux in the sensor [11]. For boundary conditions either Dirichlet ( $\Phi=\Phi_0$ ) or Neuman ( $\partial\Phi/\partial n=k$ ) boundary condition is used. No boundary condition is imposed on any 'floating' potential regions. However special measures need to be taken to tackle these regions in FE modelling. For example, a novel technique was used for the first time to simulate the 'floating' potential centre electrode in the angular position sensor shown in Figure 2(b) [12]. Since it is a conductor there must not be any electric field inside it ( $E=0$ ) and its surface must comprise an equipotential surface. This condition is satisfied by assigning an infinitely large permittivity value to all FE regions occupied by the centre electrode. Following the FE solution of the field equation (1) the capacitance  $C$  between given electrodes is calculated either from field energy  $E$  ( $E=CV^2/2$ ) for a given potential difference  $V$  or from charge  $Q$  using  $C=Q/V$ . Here the charge  $Q$  is calculated by integrating the flux density vector  $D$  over the appropriate electrode surfaces [8] using the Gauss's law:

$$Q = \oint_S D_n ds = \oint_S D \cos \theta ds = \oint_S \mathbf{D} \cdot \mathbf{n} ds = \oint_S \mathbf{D} \cdot d\mathbf{s} \quad (2)$$

Obviously any errors in the capacitance calculation are dependent upon the errors associated with the field computation and the numerical integration technique used to calculate the charge  $Q$  from equation (2). The FE models shown in Figures 3 and 4 were obtained by using the commercial FE packages OPERA-2d and OPERA-3d used for all modelling purposes [13].

## 5 SOME RESULTS OF SIMULATION

Some of the typical results of simulation in terms of equipotential contour plots and output performance characteristics are shown in Figures 5-7. Figure 5(a) clearly shows the shielding effects of the radial screens in reducing the large capacitance values between the adjacent electrodes in the 12-electrode ECT sensor. Many simulation runs involving the radial screen thickness  $\delta_4$ , its penetration depth inside the flow pipe  $\delta_3$  and the angular size of the electrodes  $\theta$  are needed to establish the optimum values of these parameters. The nonlinear effect of the flow regime on the spatial distribution of field inside the flow pipe is evident from Figure 5(b). Here, for the two-phase flow of oil (the central shaded region,  $\epsilon=3$ ) and gas (the surrounding air region,  $\epsilon=1$ ), the flow concentration  $\beta$  is defined as the ratio of the cross-sectional area of the higher permittivity component and that of the flow pipe. Figure 6 shows the typical field distribution between the outer and centre electrodes for the angular position sensor shown in Figure 2(b). The magnitude and linearity of its voltage-position

characteristic ( $V-\theta$ ) are dependent upon the uniformity of the field distribution and the position and size of the rotating electrodes [8]. As shown in Figure 7 the  $V-\theta$  characteristic is also critically dependent upon the dielectric property of the inner insulator ring ( $\epsilon_7$ ) between the centre electrode and its carrier (Figure 2(b)). Thus the stability of  $\epsilon_7$  which is sensitive to temperature variation is vitally important for the reliable performance of the sensor.

## 6 CONCLUSIONS

The generic modelling and design methodologies have been developed for capacitive sensors and the effectiveness of the adopted FE modelling strategies have been demonstrated. The modelling methodologies are applicable not only to capacitive sensors but also to other transducers and devices based on the capacitive technique.

## 7 ACKNOWLEDGEMENTS

The authors wish to thank the Engineering and Physical Sciences Research Council (EPSRC), UK for financing the work on the two capacitive sensors described in the paper. The authors would also like to acknowledge the active and close collaboration with late Professor M. S. Beck at UMIST and with Dr. C. G. Xie and Dr. S. M. Huang (formerly at UMIST) from Schlumberger Cambridge Research Limited, UK on the work on ECT sensors. Finally, the authors would like to thank Mr. T. J. Collyer (formerly at MBM Technology Limited) for his active collaboration on the work on capacitive angular position sensors.

## REFERENCES

- [1] H.U. Meyer, An integrated capacitive position sensor, *IEEE Trans. Instrum. Meas.* **45** (2) (1996) 521-525.
- [2] X. Li, G.C. M. Meijer, G. W. de Jong, and J. W. Spronck, An accurate low-cost capacitive absolute angular-position sensor with full-circle range, *IEEE Trans. Instrum. Meas.* **45** (2) (1996) 516-520.
- [3] A. Falkner, A capacitor-based device for the measurement of shaft torque, *IEEE Trans. Instrum. Meas.* **45** (4) (1996) 835-838.
- [4] X. Li and G.C.M. Meijer, A new method for the measurement of low speed using multiple-electrode capacitive sensor, *IEEE Trans. Instrum. Meas.* **46** (2) (1997) 636-639.
- [5] F.N. Toth, G.C.M. Meijer, and M. van der Lee, A planar capacitive precision gauge for liquid-level and leakage detection, *IEEE Trans. Instrum. Meas.* **46** (2) (1997) 644-646.
- [6] J.D. Kraus, Electromagnetics, 4th ed., McGraw-Hill Inc., London, 1992.
- [7] K.J. Binns, P.J. Lawrenson, and C. Trowbridge, *The Analytical and Numerical Solution of Electric and Magnetic Fields*, John Wiley & Sons, Chichester, 1992.
- [8] S.H. Khan and F. Abdullah, Finite element modelling of multielectrode capacitive systems for flow imaging, *IEE Proceedings-G*, **140** (3) (1993) 216-222.
- [9] M.S. Beck, A. Plaskowski, and R.G. Green, Imaging for measurement of two-phase flows, in: *Proceedings of the 4th International Symposium on Flow Visualization*, 1986, p. 585-588.
- [10] M.S. Beck, B.S. Hoyle, and C.P. Lenn, Process tomography in pipelines, *SERC Bulletin*, **4** (10) (1992) 24-25.
- [11] S.H. Khan, K.T.V. Grattan, and L. Finkelstein, Investigation of leakage flux in a capacitive angular displacement sensor used in torque motors by 3D finite element field modelling, *Sensors and Actuators: A. Physical*, **76** (1999) 253-259.
- [12] S.H. Khan, L. Finkelstein, and F. Abdullah, Investigation of the effects of design parameters on output characteristics of capacitive angular displacement sensors by finite element field modelling, *IEEE Trans. on Magnetics*, **33** (2) (1997) 2081-2084.
- [13] OPERA-2d, version 7.035 1998, OPERA-3d version 2.609 and TOSCA version 6.6, 1997, Vector Fields Limited, UK

**AUTHORS:** Dr. Sanowar H. KHAN, Professor Kenneth T.V. GRATTAN and Professor Ludwik FINKELSTEIN, Measurement and Instrumentation Centre, Department of Electrical, Electronic and Information Engineering, City University, Northampton Square, London EC1V 0HB, UK, Telephone: +44 (0)20 7477 8183, Fax: +44 (0)20 7477 8568, Email: [S.H.Khan@city.ac.uk](mailto:S.H.Khan@city.ac.uk)